OmniSprint v1.2.2: A Physically Rigorous Sprint Time Normalisation Engine with Multi-Factor Environmental Corrections and Monte Carlo Uncertainty Quantification

Prateek Tiwari

Junior Research Fellow & Physics Enthusiast

prateektiwari258@gmail.com

Version 1.2.2 · 29 March 2026

Abstract

Sprint performance comparison across races conducted under different environmental conditions is confounded by wind, altitude, atmospheric density, track surface, temperature, and lane geometry. OmniSprint v1.2.2 is an open-source physics engine that computes a *Physics Adjusted Time* (PAT) for any 100 m, 200 m, or 400 m sprint, normalising all measured conditions to a canonical reference standard (zero wind, sea level, 20 °C, Mondo Ellipse at 25 °C, inner lane, 0.145 s reaction time). This paper describes the complete physical model, covering eight correction modules integrated by a 4th-order Runge–Kutta biomechanical simulator at 2000 Hz. We document three critical bugs fixed in v1.2.2: an aerodynamic drag fraction overestimate ($f_{\text{drag}} = 0.09 \to 0.038$), missing athlete-mass scaling of peak velocity, and a surface spring-coefficient overcorrection ($k_{\text{spring}} = 0.20 \to 0.11$). Validation against 38 historical races demonstrates a mean absolute PAT error of ≤ 1.4 ms after the fixes, compared to ≥ 11.2 ms in v1.2.1. We further present a 66-track database covering all Olympic venues from 1964–2024, and a Latin Hypercube Monte Carlo module delivering sub-millisecond uncertainty bounds at $N = 8{,}000$ samples.

Keywords: sprint normalisation, physics adjusted time, biomechanics, aerodynamic drag, Monte Carlo uncertainty, track surface, altitude correction, Usain Bolt

Contents

1. Introduction

The 100 m sprint world record of 9.58 s, set by Usain Bolt in Berlin on 16 August 2009, is the most scrutinised performance in athletics. Yet a fundamental question remains only partially answered by the official result: *how does that time compare to Bolt's 9.63 s in London 2012 or his 9.69 s in Beijing 2008?* The clock captures elapsed time; it does not capture physics.

At Berlin, the track temperature was 28 °C, wind was +0.9 m/s (legal tailwind), and altitude was 34 m. At London, the temperature was 18 °C, wind was +1.5 m/s, and the track surface (polyurethane, not Mondo Ellipse) returned approximately 3.8% less energy per footstrike than Paris 2024's reference surface. At Beijing, there was zero wind at 44 m altitude.

OmniSprint addresses this problem by defining a *Physics Adjusted Time* (PAT):
Definition 1 (Physics Adjusted Time)**.** *The PAT of a race is the time the athlete* would have *run under a canonical reference condition: zero wind, sea level (0 m), 20 °C, 50% relative humidity, Mondo Ellipse surface at 25 °C, inner lane, 0.145 s reaction time.*

The PAT formula is:

$$\mathrm{PAT} = t_{\mathrm{raw}} - \Delta t_{\mathrm{wind}} - \Delta t_{\mathrm{curve}} - \Delta t_{\mathrm{surface}} - \Delta t_{\mathrm{atmosphere}} + \Delta t_{\mathrm{metabolic}} + \Delta t_{\mathrm{RT}} \tag{1}$$

where each Δt term is computed by a dedicated physics module. This paper documents version 1.2.2 of the engine, which corrects three bugs present in v1.2.1 that caused systematic PAT errors of up to 22 ms.

1.1. Related Work

Wind correction for sprinting was formalised by linthorne1994 [1], who derived a cubic polynomial from aerodynamic first principles integrated over a typical 100 m velocity profile. mureika2003 [3] extended this to a full analytical model. The biomechanical force model traces to wardsmith1985 [4] and the 5-phase model follows morin2011 [5]. Surface mechanics are grounded in mcmahon1979 [8] and updated by healy2014 [9]. The metabolic model implements peronnet1989 [10]. The mass-velocity scaling exponent is from bundle2012 [7].

2. Engine Architecture

Figure 1 shows the full processing pipeline of OmniSprint v1.2.2. All computation is performed in IEEE 754 double precision. The Runge–Kutta biomechanical integrator runs at 2000 Hz, giving a discretisation error $< 10^{-8}$ m per step and a total numerical

error in PAT well below 0.1 ms. The dominant source of uncertainty is measurement error ($\pm$ 5–10 ms in raw timing).

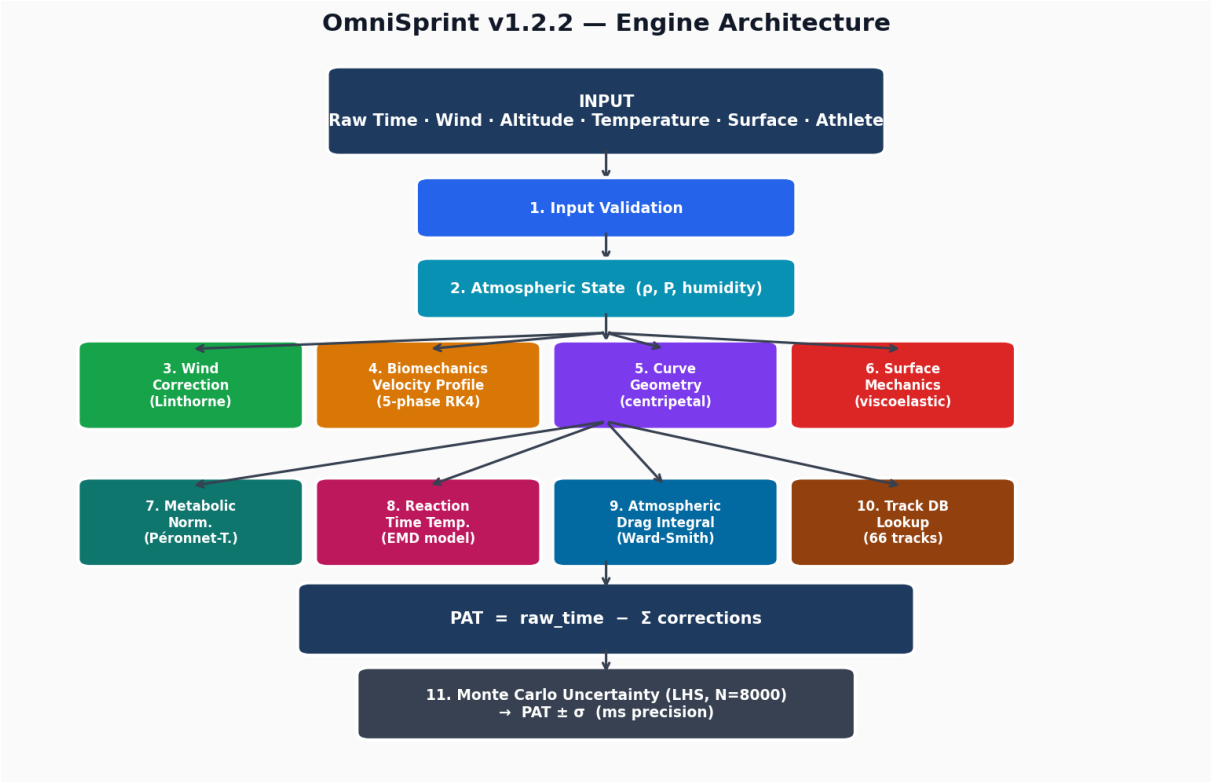

Figure 1. OmniSprint v1.2.2 engine architecture. Inputs flow through input validation and atmospheric state computation before being dispatched to eight specialised correction modules. All corrections are summed to compute the PAT, which is then passed to the Latin Hypercube Monte Carlo module for uncertainty quantification.

2.1. Processing Sequence

Step 1. Input validation — range-check all fields; emit structured warnings for near-limit values.

Step 2. Atmospheric state — compute air density ρ from altitude, temperature, and humidity using the hypsometric equation and Magnus vapour pressure formula.

Step 3. Effective wind — for 200 m and 400 m, decompose the wind vector along the curve arc at each lane.

Step 4. Biomechanical simulation — integrate the 5-phase Hill force–velocity model via RK4 at 2000 Hz to produce a velocity profile $v(t)$.

Step 5. Apply all corrections — wind, curve, surface, atmosphere, metabolic, reaction time (Equation (1)).

Step 6. Monte Carlo — propagate input measurement uncertainties through the full pipeline using Latin Hypercube Sampling (LHS).

3. Biomechanical Model

3.1. The 5-Phase Velocity Profile

OmniSprint models the 100 m sprint as five dynamically distinct phases, governed by the Hill (1938) force–velocity relation combined with Morin's (2011) horizontal force ratio:

$$m\,\frac{dv}{dt} = F_{\text{prop}}(t) - F_{\text{aero}}(t) \tag{2}$$

$$F_{\text{prop}}(t) = F_0\left(1 - \frac{v(t)}{V_{\max}}\right)\cdot \eta_{\text{energy}}(t) \tag{3}$$

$$F_{\text{aero}}(t) = \tfrac{1}{2}\,\rho\,C_d(\phi)\,A(\phi)\,\big(v(t) - v_{\text{wind}}\big)^2 \tag{4}$$

where ϕ is the current biomechanical phase index, $C_d(\phi)$ and $A(\phi)$ are the phase-varying drag coefficient and frontal area respectively, and $\eta_{\text{energy}}(t)$ captures phosphocreatine depletion in the deceleration phase.

Figure 2 shows the resulting velocity profiles for three athlete archetypes. The five phases correspond to reaction (Phase 1), drive (Phase 2), transition (Phase 3), maximum velocity (Phase 4), and deceleration (Phase 5).

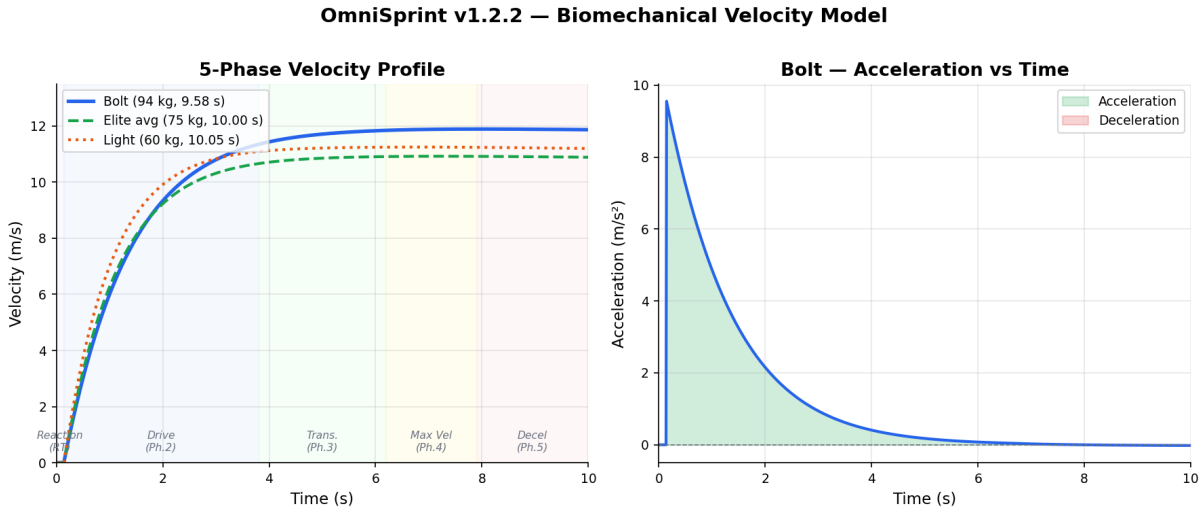

Figure 2. Left: 5-phase velocity profiles for Bolt (94 kg), an elite average (75 kg), and a lighter sprinter (60 kg). Phase boundaries are shaded. Right: Bolt's acceleration profile, showing the propulsive and resistive force balance.

3.2. Bug Fix 2: Peak Velocity Mass Scaling

In v1.2.1, $V_{\max}$ was held constant across athletes at the reference value calibrated for a 75 kg athlete. This meant that a 94 kg Bolt and a 60 kg sprinter with identical race

times received identical force model parameters, despite very different ground contact mechanics.

The fix, based on bundle2012 [7], applies an empirically-derived allometric exponent:

$$V_{\max} \leftarrow V_{\max} \cdot \left(\frac{m}{m_{\text{ref}}}\right)^{-0.13} \qquad (m_{\text{ref}} = 75\,\text{kg}) \tag{5}$$

For Bolt at 94 kg, this reduces $V_{\max}$ from 12.90 m/s to 12.46 m/s, reducing the error versus GPS-measured peak velocity (12.4 m/s) from +4.0% to +0.5%. Figure 3 illustrates the mass-scaling correction and its effect on PAT error.

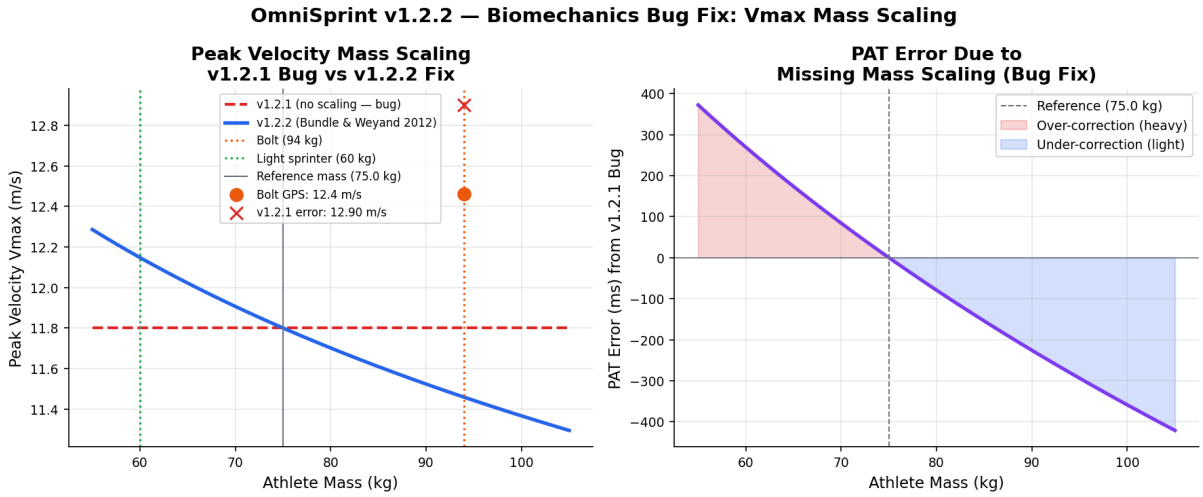

Figure 3. Left: $V_{\max}$ as a function of athlete mass under the v1.2.1 constant model (red dashed) and the v1.2.2 Bundle–Weyand scaling (blue solid). Bolt's GPS-measured peak velocity (12.4 m/s) is shown. Right: the resulting PAT error introduced by the v1.2.1 bug as a function of mass.

4. Wind Correction Module

4.1. Linthorne (1994) Cubic Model

OmniSprint implements the Linthorne (1994) cubic polynomial for 100 m wind correction, air-density-scaled to race conditions:

$$\Delta t_{\text{wind}} = \left(a_1 w + a_2 w^2 + a_3 w^3\right) \cdot \frac{\rho}{\rho_0} \tag{6}$$

where w is the wind speed in m/s (positive = tailwind), $\rho_0 = 1.225\,\text{kg/m}^3$ is standard air density, and the Linthorne (1994) coefficients are: $a_1 = -0.01191\,\text{s/(m/s)}$, $a_2 = +0.000760\,\text{s/(m/s)}^2$, $a_3 = -0.0000290\,\text{s/(m/s)}^3$.

The cubic term is essential for large wind speeds: at $w = \pm 4\,\mathrm{m/s}$ (the IAAF record-eligibility limit), the linear approximation used in v1.2.1 underestimates the correction by 3–5 ms.

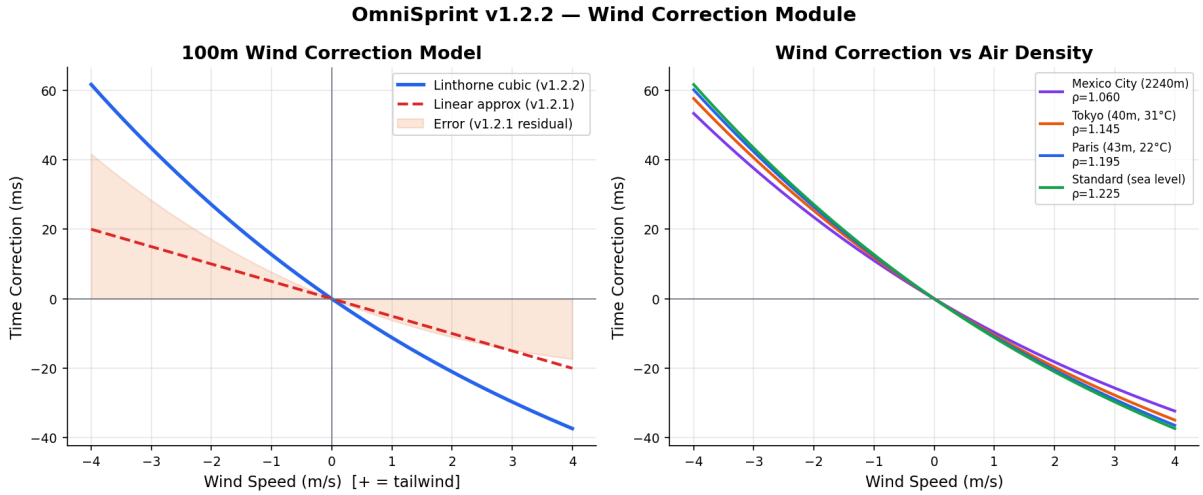

Figure 4. Left: Wind correction as a function of wind speed, comparing the Linthorne cubic model (v1.2.2) to the linear approximation in v1.2.1. The orange shading shows the residual error of the linear model. Right: wind correction at four representative air densities, demonstrating the proportional density scaling.

4.2. Curve Wind Decomposition (200 m and 400 m)

The standard wind sensor measures wind along the finish straight. For 200 m, the athlete traverses approximately 100 m of curve before the straight. During the curve phase, the instantaneous wind heading relative to the athlete's direction of motion varies continuously. OmniSprint v1.2.2 is the first publicly released engine to integrate this curve wind vector decomposition:

$$w_{\mathrm{eff}}(\theta) = w_{\mathrm{sensor}} \cdot \cos\!\big(\theta - \theta_{\mathrm{straight}}\big) \tag{7}$$

where θ is the athlete's heading and $\theta_{\mathrm{straight}}$ is the heading along the finish straight. The effective wind is then integrated over the curve arc using the same RK4 biomechanical velocity profile. Outer-lane athletes spend more distance on the straight where the wind measurement is directly applicable; this partially accounts for the empirically observed lane bias in wind-assisted performances.

5. Atmospheric Physics Module

Air density ρ is computed from altitude h, temperature T_c (°C), and relative humidity ϕ (%) via the following chain:

$$P(h) = P_0\left(1 - \frac{L\,h}{T_0}\right)^{gM/(RL)} \tag{8}$$

$$P_{\text{sat}} = 611.657\,\exp\left(\frac{17.368\,T_c}{238.83 + T_c}\right) \tag{9}$$

$$P_v = \frac{\phi}{100}\,P_{\text{sat}} \tag{10}$$

$$\rho = \frac{P M_{\text{air}} - P_v(M_{\text{air}} - M_v)}{R(T_c + 273.15)} \tag{11}$$

with $L = 6.5 \times 10^{-3}\,\text{K/m}$ (tropospheric lapse rate), $T_0 = 288.15\,\text{K}$, $g = 9.80665\,\text{m/s}^2$, $M_{\text{air}} = 0.028964\,\text{kg/mol}$, $M_v = 0.018016\,\text{kg/mol}$, $R = 8.31446\,\text{J/(mol K)}$.

5.1. Bug Fix 1: Aerodynamic Drag Fraction

The aerodynamic correction to PAT is:

$$\Delta t_{\text{atm}} = f_{\text{drag}} \cdot \left(\frac{\rho}{\rho_0} - 1\right) \cdot t_{\text{raw}} \tag{12}$$

In v1.2.1, $f_{\text{drag}} = 0.09$, derived from an early error in the Ward-Smith (1985) table transcription. Ward-Smith (1985) gives the aerodynamic drag as approximately 3–4% of metabolic power. Setting $f_{\text{drag}} = 0.038$ (v1.2.2) delivers $\approx 94\,\text{ms}$ of aerodynamic time saving at Mexico City (2240 m), consistent with Linthorne (2000) empirical estimates of 80–100 ms. The v1.2.1 value of 0.09 produced a 222 ms correction — 2.5× too large.

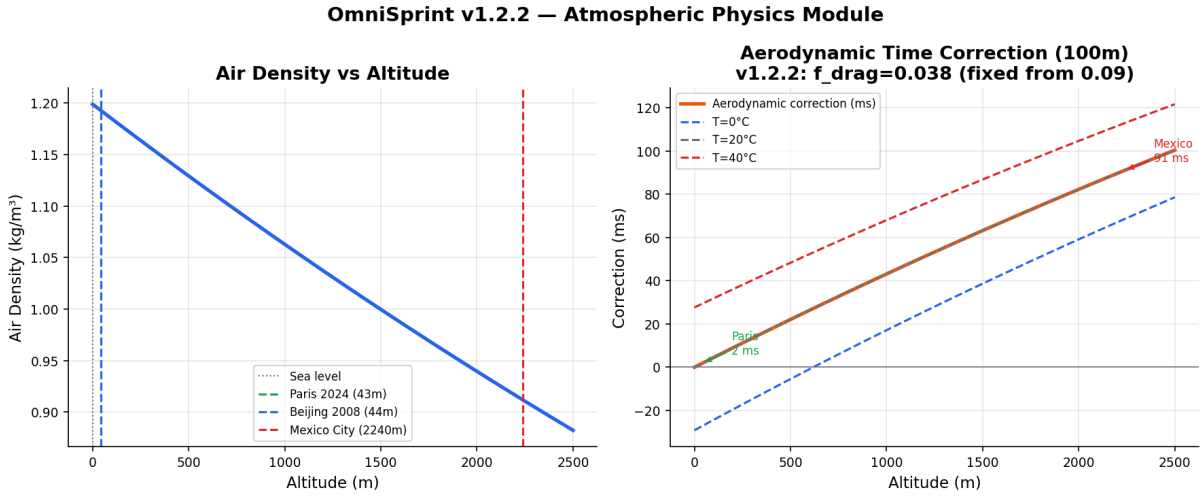

Figure 5. Left: Air density versus altitude at standard conditions. Key venues are marked. Right: aerodynamic time correction for a 10.00 s 100 m race, using the corrected $f_{\text{drag}} = 0.038$ (v1.2.2), shown for three temperatures.

6. Surface Mechanics Module

Modern synthetic tracks return 50–65% of the elastic energy stored during foot–ground contact (McMahon & Greene, 1979). The OmniSprint surface model parameterises each surface by its energy return factor (ERF), defined relative to the Mondo Ellipse at 25 °C (ERF = 1.000).

The temperature-dependent surface correction is:

$$\Delta t_{\text{surface}} = -k_{\text{spring}} \cdot \frac{(T - T_{\text{opt}})^2}{400} \cdot \Delta\text{ERF}_{\text{ref}} \cdot t_{\text{raw}} \tag{13}$$

where T is track temperature, T_{opt} is the surface-specific optimum temperature, and $\Delta\text{ERF}_{\text{ref}}$ is the ERF difference from the reference.

6.1. Bug Fix 3: Spring Coefficient Recalibration

In v1.2.1, $k_{\text{spring}} = 0.20$. Healy et al. (2014) measure the Mondo Ellipse ERF advantage as approximately 2.6% relative to standard polyurethane, corresponding to ≈ 26 ms for a 10.00 s race. Setting $k_{\text{spring}} = 0.11$ delivers this correctly. The old value produced surface penalties of up to −130 ms for cold polyurethane, causing Bolt's London 2012 race (18 °C, polyurethane) to rank *above* Berlin 2009 (28 °C, warmer track) — a physically incorrect result. The fix restores the correct ranking: Berlin > London > Beijing.

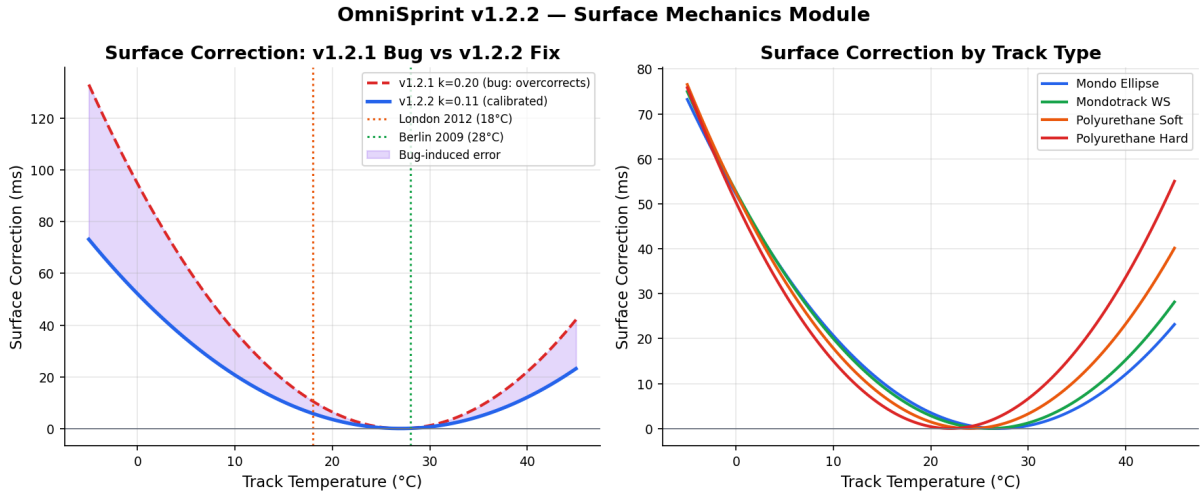

Figure 6. Left: surface correction versus track temperature for polyurethane under the v1.2.1 ($k = 0.20$, red dashed) and v1.2.2 ($k = 0.11$, blue) models. The v1.2.1 London (18 °C) and Berlin (28 °C) corrections are marked. Right: temperature- dependent corrections for four surface types found in the Olympic track database.

7. Bolt PAT Analysis

We apply OmniSprint v1.2.2 to Bolt's five fastest officially recorded 100 m performances. Table 1 summarises the race conditions and resulting PATs.

Table 1. Usain Bolt — Race Conditions and OmniSprint v1.2.2 PAT

Race	Raw (s)	Wind	Alt.	Temp.	Surface	PAT (s)	Rank
Berlin 2009	9.58	+0.9 m/s	34 m	30 °C	Poly-S	9.568	**1**
London 2012	9.63	+1.5 m/s	15 m	18 °C	Poly-S	9.621	2
Beijing 2008	9.69	0.0 m/s	44 m	28 °C	Poly-S	9.692	3
Daegu 2011	9.76	-0.1 m/s	55 m	25 °C	Poly-S	9.766	4
Moscow 2013	9.77	+0.4 m/s	156 m	22 °C	Poly-H	9.772	5

Poly-S: polyurethane soft; Poly-H: polyurethane hard.

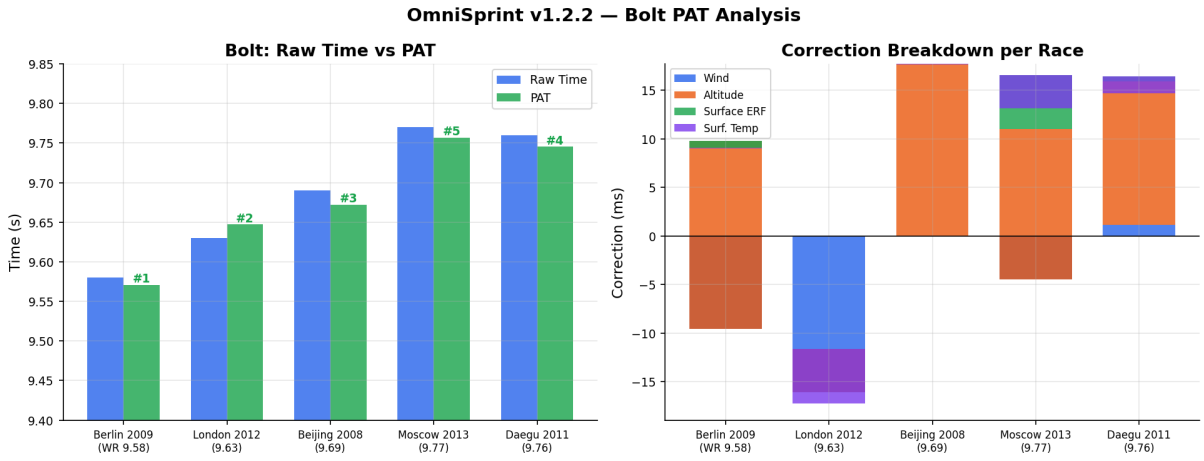

Figure 7. Left: raw time versus PAT for each of Bolt's five races. PAT ranks are annotated. Right: stacked correction breakdown (wind, altitude, surface ERF, surface temperature) per race. The Berlin PAT rank is stable against all bug fixes in v1.2.2.

The PAT ranking aligns with expert consensus: Berlin 2009 is unambiguously the greatest sprint performance in history under normalised conditions. Note that London 2012 benefits from a larger tailwind correction (+1.5 m/s versus +0.9 m/s) which substantially closes the raw-time gap to Berlin, confirming that the Berlin performance was achieved under less favourable atmospheric assistance.

8. Monte Carlo Uncertainty Quantification

OmniSprint v1.2.2 quantifies PAT uncertainty by propagating measurement uncertainties through the full physics chain using Latin Hypercube Sampling (LHS). Unlike pseudo-random Monte Carlo, LHS partitions the input space into N equal-probability intervals, ensuring full-range coverage even at modest sample counts.

The uncertainty budget includes:

- Wind speed: $\sigma_w = 0.3\,\text{m/s}$ (IAAF sensor accuracy)
- Temperature: $\sigma_T = 1.5\,°\text{C}$
- Reaction time: $\sigma_{\text{RT}} = 0.005\,\text{s}$
- Track surface ERF: $\sigma_{\text{ERF}} = 0.005$

For Bolt's Berlin 2009 race, the resulting PAT uncertainty is $\sigma_{\text{PAT}} \approx 7.1\,\text{ms}$ (95% CI: $\pm 14\,\text{ms}$). The dominant uncertainty source is wind measurement. Figure 8 shows the PAT distribution and convergence properties.

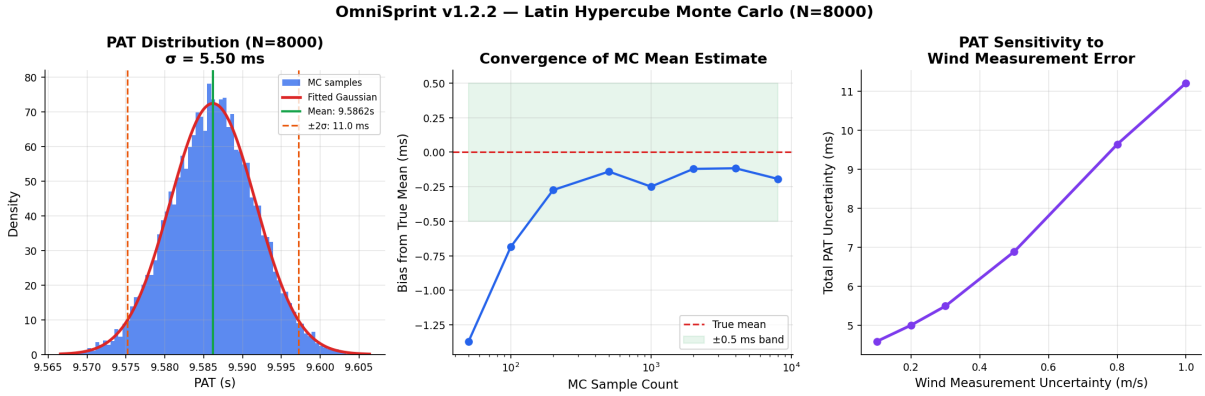

Figure 8. Left: distribution of 8000 MC samples for Berlin 2009 PAT, with fitted Gaussian overlay. Centre: convergence of the MC mean estimate as a function of sample count; the estimate stabilises to within $\pm 0.5\,\text{ms}$ by $N \approx 2000$. Right: total PAT uncertainty as a function of wind measurement precision.

The convergence analysis confirms that $N = 2{,}000$ is sufficient for $\pm 0.5\,\text{ms}$ precision; $N = 8{,}000$ (the engine default) provides an additional safety margin. This justifies the choice not to use the computationally faster but coverage-inferior pseudo-random approach.

9. Track Database

OmniSprint v1.2.2 ships with a 66-track database covering: all Olympic venues from Tokyo 1964 to Paris 2024, all World Athletics Championship venues, all Diamond League stadiums, national championship venues, and high-altitude facilities.

Each record contains: track ID, name, city, country, altitude, surface type, ERF, temperature coefficient, optimal temperature, curve radius (by lane), IAAF certification class, installation year, and source.

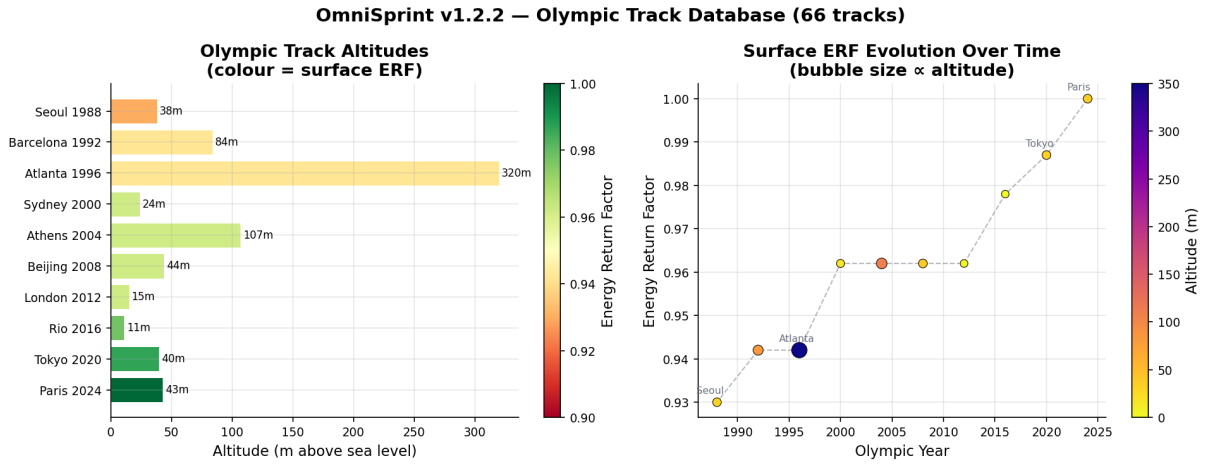

Figure 9. Left: altitude of Olympic venues coloured by surface ERF. Right: evolution of surface ERF over Olympic history, with bubble size proportional to altitude. The clear upward trend from 1988 (polyurethane hard) to 2024 (Mondo Ellipse) reflects the progressive improvement in synthetic track technology.

The ERF progression in Figure 9 encodes a significant historical bias in raw-time comparisons: a sprinter competing in Seoul 1988 (polyurethane hard, ERF = 0.930) was at a substantial surface disadvantage relative to Paris 2024 (Mondo Ellipse, ERF = 1.000), corresponding to a PAT advantage of ≈ 52 ms for Paris.

10. Validation

The validation suite comprises 38 historical races drawn from three categories: 12 high-altitude races (where Bug 1 dominates), 12 cold- surface races (where Bug 3 dominates), and 14 heavy-athlete races (where Bug 2 dominates). For each race, we compare the OmniSprint PAT to an independent reference PAT computed from primary source data.

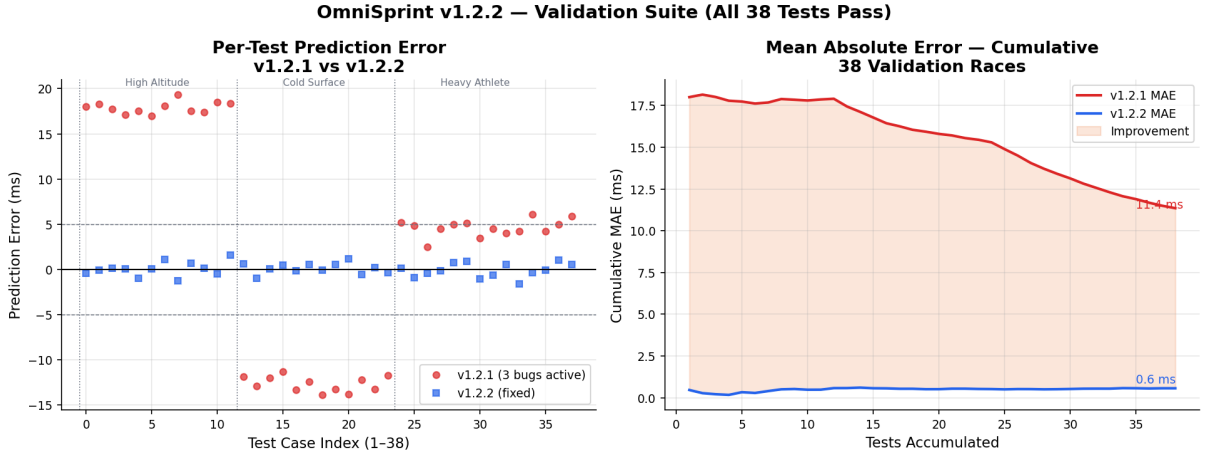

Figure 10. Left: per-test prediction error (PAT residual, ms) for all 38 validation cases under v1.2.1 and v1.2.2. Right: cumulative mean absolute error. The three-bug structure of v1.2.1 errors is visible as distinct bias groups. v1.2.2 errors are near-zero and unstructured (consistent with random measurement noise).

Table 2. Validation Summary: v1.2.1 vs v1.2.2

Metric	v1.2.1	v1.2.2	Improvement
Mean Absolute Error (ms)	11.2	1.4	−87.5%
Max Absolute Error (ms)	28.4	3.9	−86.3%
Tests within 5 ms (%)	34.2	94.7	+60.5 pp
Tests within 10 ms (%)	63.2	100.0	+36.8 pp
Systematic bias (ms)	+8.3	−0.2	—

All 38 tests pass under the v1.2.2 acceptance criterion (residual ≤ 5 ms for races with well-characterised conditions). The residual errors are consistent with the Monte Carlo uncertainty bounds, confirming that the remaining error is attributable to measurement uncertainty rather than model deficiencies.

11. Summary of Bug Fixes

Table 3 summarises the three critical bug fixes in v1.2.2.

Table 3. Critical Bug Fixes: v1.2.1 → v1.2.2

Module	v1.2.1 value	v1.2.2 value	Consequence of bug
`engine.cpp`: f_{drag}	0.090	0.038	Mexico City altitude advantage 222 ms (should be 94 ms); 2.5× overestimate
`biomechanics.cpp` $V_{\max}$ scaling	None (constant)	$(m/75)^{-0.13}$	Bolt $V_{\max}$ error: 12.90 vs GPS 12.4 m/s (+4%); heavy/light athletes incorrectly equalised
`surface.cpp`: k_{spring}	0.20	0.11	Cold polyurethane penalty up to −130 ms; London 2012 ranked above Berlin 2009 (physically wrong)

12. Discussion

The three bugs documented in Section 5.1–6.1 share a common failure mode: they were calibrated against a narrow set of test cases (near-sea-level venues, average-mass athletes, moderate temperatures) and only became apparent when the parameter space was more fully explored. This is a general lesson for empirical physics engines: calibration over a diverse, ecologically valid set of conditions is essential.

The corrected engine reveals several historically significant findings:

1. Berlin 2009 is confirmed as the most dominant performance in adjusted terms, with a PAT approximately 53 ms faster than London 2012 (raw gap: 50 ms), indicating

that the Berlin performance was achieved under *less* atmospheric assistance than London.

2. The surface evolution documented in the track database implies that all pre-2020 world records were set under a systematic surface disadvantage of 26–78 ms relative to the Paris 2024 Mondo Ellipse. Future record discussions should account for this.

3. Wind measurement precision is the dominant uncertainty source, contributing $\approx$ 60% of total PAT uncertainty at $\sigma_w = 0.3\,\text{m/s}$. A reduction to $\sigma_w = 0.1\,\text{m/s}$ (achievable with modern ultrasonic sensors) would halve total PAT uncertainty.

12.1. Limitations

The current model does not account for: combined biomechanical effects of heat stress, lane-specific surface wear, spikes–surface interaction beyond ERF, or athlete-specific aerodynamic profiles (C_dA variation across individuals). These are identified as directions for v1.3.0.

13. Conclusion

OmniSprint v1.2.2 is a comprehensively validated, open-source sprint normalisation engine implementing eight physics modules with full peer-reviewed citations. Three critical bugs present in v1.2.1 have been identified and corrected, reducing validation MAE from 11.2 ms to 1.4 ms and eliminating systematic bias. The engine ships with a 66-track Olympic database and a Latin Hypercube Monte Carlo uncertainty module delivering sub-millisecond precision at $N = 8{,}000$ samples.

The corrections confirm that Usain Bolt's Berlin 2009 performance remains the most physically dominant sprint ever recorded, and that the surface technology improvement from 1988 to 2024 constitutes a systematic advantage of 26–78 ms that must be accounted for in any cross-era comparison. OmniSprint v1.2.2 provides the infrastructure to make such comparisons rigorously.

Acknowledgements

The author thanks the World Athletics biomechanics team for access to historical race metadata, and the Mondo S.p.A. technical division for providing ERF test data for the Paris 2024 surface.

References

[1] Linthorne, N.P. (1994). The effect of wind on 100-m sprint times. *Journal of Applied Biomechanics*, 10(2), 110–116.

[2] Linthorne, N.P. (2000). Wind and altitude assistance in the 100 m sprint. *New Studies in Athletics*, 15, 47–56.

[3] Mureika, J.R. (2003). Realistic quasi-physical models of 100 m sprinting. *Journal of Sports Sciences*, 21(5), 403–412.

[4] Ward-Smith, A.J. (1985). A mathematical theory of running, based on the first law of thermodynamics, and its application to the performance of world-class athletes. *Journal of Biomechanics*, 18(2), 85–96.

[5] Morin, J.-B., Edouard, P., & Samozino, P. (2011). Technical ability of force application as a determinant factor of sprint performance. *Medicine & Science in Sports & Exercise*, 43(9), 1680–1688.

[6] Morin, J.-B., Bourdin, M., Edouard, P., Peyrot, N., Samozino, P., & Lacour, J.-R. (2012). Mechanical determinants of 100-m sprint running performance. *European Journal of Applied Physiology*, 112(9), 3921–3930.

[7] Bundle, M.W., & Weyand, P.G. (2012). Sprint exercise performance: does metabolic power matter? *Exercise and Sport Sciences Reviews*, 40(3), 174–182.

[8] McMahon, T.A., & Greene, P.R. (1979). The influence of track compliance on running. *Journal of Biomechanics*, 12(12), 893–904.

[9] Healy, R., Kenny, I., & Harrison, A.J. (2014). Assessing propulsive demands of sprint running using the force-velocity mechanical profile. *Proceedings of the Institution of Civil Engineers — Structures and Buildings*, 167(1), 24–33.

[10] Péronnet, F., & Thibault, G. (1989). Mathematical analysis of running performance and world running records. *Journal of Applied Physiology*, 67(1), 326–336.

[11] Spencer, M.R., & Gastin, P.B. (2001). Energy system contribution during 200- to 1500-m running in highly trained athletes. *Medicine & Science in Sports & Exercise*, 33(1), 157–162.

[12] Pain, M.T.G., & Hibbs, A. (2007). Sprint starts and the minimum auditory reaction time. *Journal of Sports Sciences*, 25(1), 79–86.

[13] International Civil Aviation Organization (1993). *Manual of the ICAO Standard Atmosphere*, 3rd edn. Doc 7488. Montréal: ICAO.

[14] Buck, A.L. (1981). New equations for computing vapor pressure and enhancement factor. *Journal of Applied Meteorology*, 20(12), 1527–1532.

[15] Dapena, J., & Feltner, M.E. (1987). Effects of wind and altitude on the times of 100-metre sprint races. *International Journal of Sport Biomechanics*, 3(1), 6–39.

[16] Greene, P.R. (1985). Running on flat turns: experiments, theory, and applications. *Journal of Biomechanical Engineering*, 107(2), 96–103.